Korean J. Chem. Eng., 36(7), 1115-1123 (2019)
DOI: 10.1007/s11814-019-0292-0

pISSN: 0256-1115
eISSN: 1975-7220

Thermodynamic and kinetic studies sorption of 5-fluorouracil onto single walled carbon nanotubes modified by chitosan

Samane Karimidost, Elham Moniri†, and Mahsasadat Miralinaghi

Department of Chemistry, Varamin (Pishva) Branch, Islamic Azad University, Varamin, Iran
(*Received 8 October 2018 • accepted 7 May 2019*)

Abstract−Single-walled carbon nanotubes (SWCNTs) were functionalized by chitosan and their application was examined in adsorbing an anti-cancer drug, 5-fluorouracil (5Fu). Surface, physical and morphological characteristics of raw SWCNTs and Chitosan-functionalized SWCNTs (Ch-SWCNTs) were extensively characterized by Fourier transform spectroscopy (FTIR), field emission scanning electron microscopy (FESEM), thermogravimetric analysis (TGA), Brunauer-Emmet-Teller (BET) and X-ray diffraction (XRD). The effects of various variables such as pH, initial drug concentration, temperature, and contact time on adsorption capacity were also investigated. Thermodynamic parameters such as ΔS^o, ΔH^o, and ΔG^o were estimated. Isotherm and kinetic studies of drug adsorption indicated that the adsorption process followed Langmuir isotherm model and pseudo-second-order kinetic, respectively. The maximum adsorption capacity (q_m) of 5Fu on Ch-SWCNTs was 31.77 mg g^{-1} at 298 K, pH 4.0, and 120 min, which is higher than adsorption capacity of SWCNTs (4.12 mg g^{-1}) in the same conditions. The adsorption was spontaneous and exothermic process in nature, with a slight decreasing in entropy.

Keywords: Anti-cancer Medicine, Nano-carrier, Single-walled Carbon Nanotube

INTRODUCTION

Targeting and drug delivery to inaccessible parts of human body using nonmetric equipment is a main application of nanotechnology in medical sciences. Precise and effective transmission of drugs to certain targets requires operating systems smaller than the target. The widely-used methods of drug analysis in biological samples and also delivery system are based on nano-magnetic carrier [1-5]. In spite of that, among well-known drug carriers are micelles, liposomes, den dimers, hydrogels and nanomaterial [6].

Because of small size, nanomaterials can diffuse cellular barriers (such as membranes) into the cell and only influence cells of the considered tissue by target perception accumulation [7]. Moreover, therapeutic factors can be placed on the surface of nanomaterial so that immune system may not recognize them [8]. Since 2004, carbon nanotubes have been widely considered by researchers as nano scale drug carriers capable of intercellular transmission of chemotherapy drugs, proteins and genes. Unique structural, physical and chemical features of nanotubes make them promising substances in a wide range of modern cancer therapies such as photodynamic therapy, photo-thermal therapy, photo-acoustic therapy and tumor eradication through radio waves [9,10].

A main constraint in application of carbon nanotubes (CNTs) in biomedical therapies is their insolubility in aqueous environments and other solvents, reducing biocompatibility of such materials [11]. Chemical modification and functionalization of CNTs facilitates their spread in water and physiological environments. To date, several strategies have been developed to reinforce biocompatibility and solubility of CNTs, some of which include oxidation [12], modification with small organic compounds [13] or polymers [14], and dispersion with surface active biocompatible materials [15]. Polymer-modified CNTs are considered effective potential carriers of intelligent drug-delivery systems. Among biopolymers, chitosan (Ch) is a linear cationic among polysaccharide composed of α-D-glucosamine, which is obtained by partial diacetylation of chitin (one of the most frequent biopolymers in nature) in alkali conditions. Because of its non-toxic, hydrophilic, compatibility and biodegradability features and having frequent amine and hydroxyl groups, chitosan is of great importance in preparing drug-carriers with favorable biocompatibility and controlled behavior in biological systems [16-18]. So, the combination of chitosan and SWCNT or modification of graphene family with chitosan [19] can be useful for so many fields, especially for study of drug delivery.

Jang et al. developed a drug-delivery system involving SWCNTs modified with sodium alginate polysaccharides, chitosan, and folic acid (FA) for controlled delivery of doxorubicin (DOX), an anti-cancer drug [20]. The link between FA and SWCNT led to exclusive transfer of DOX into heal cell liposomes and enhance its performance compared to DOX alone. Lee et al functionalized MWCNTs (multi-walled carbon nanotubes) with chitosan oligomers (with molecular weight of 400-600 DA) in a covalent manner to improve their solubility. Then, they connected tea polyphenols to it by establishing a hydrogen bond. The rate of drug-delivery from the carrier could be controlled by changing the pH and gamma radiation. Because of their higher strength and less toxicity compared to MWCNTs, SWCNTs have wider applications in nano medicine [21].

5FU is a chemotherapy factor used in treatment of many diseases. This drug exerts a cytotoxic effect as an antimetabolite and

†To whom correspondence should be addressed.
E-mail: moniri30003000@yahoo.com

competes an important enzyme in thymidine composition. Therefore, 5FU controls DNA synthesis.

The objective of this research was to prepare a nano-composite capable of loading 5FU through adsorption. Hence, raw SWCNTs were oxidized by HCl Treatment and then functionalized by Ch biopolymer. Types of functional groups, surface features, crystalline structure and thermal stability of Ch-SWCNT were studied using FTIR, FE-SEM, BET, XRD and TGA methods. Adsorption behavior of 5FU including kinetics, isothermal, thermodynamic and adsorption mechanism, and potential effective factors on 5FU adsorption process were investigated and results were analyzed. The presented research can be applied to drug delivery system and also environmental fields for removal of the drug from west water of pharmaceutical industries.

MATERIALS AND METHODS

1. Material

Single-walled carbon nanotubes (SWCNTs in chief, purity=98 wt%, diam. 1.6-8 nm, length 5-30 μm) were purchased from Nano Research Co. (US). Chitosan with 91% degree of deacetylation (DD) and 2.1×105 of molecular weight and 5Fu ($C_4H_3FN_2O_2$) (130.8 $g \cdot mol^{-1}$) and the other reagents of analytical grade (such as hydrochloric acid, boric acid, phosphoric acid, petroleum ether, dioxin, xylene, and cyanuric chloride were purchased from Sigma (Germany). All reagents were used without further treatment.

2. Instrumental

FT-IR spectroscopy measurements were conducted by using Vector 22 spectrometer in KBr pellet in the range of 4,000-400 cm^{-1} at room temperature (Bruker Co. America). The Brunauer-Emmett-Teller (BET) surface areas of samples were measured by N_2 adsorption-desorption isotherms at 77 K on a Micromeritics ASAP2020 model (America). Thermogravimetric analyses (TGA) of samples were recorded from room temperature to 600 °C at a heating rate of 10 °C/min under a 107 nitrogen atmosphere by an STA 1500 thermogravimetric analyzer (Rheometric Scientific Co. America). The morphology of materials was studied by field emission scanning electron microscope (FESEM) (Sigma, Zeiss Co. Germany). X-ray powder diffraction (XRD) patterns were performed on a Star model, diffractometer operating with Cu Kα source (λ=1.541 Å) (Stoe Co. Germany). A single beam UV-Vis spectrometer was employed to determine maximum wavelength (λ_{max}=269 nm) (DR2800 model, America). The pH values of aqueous solutions were adjusted by metrohm pH meter (America).

3. Preparation of Chitosan-functionalized SWCNTs (Ch-SWCNTs)

First, 1 g of raw SWCNTs was dispersed in 100 mL HCl (1%) under stirring at room temperature for 24 h. Pure oxidized SWCNTs (OX-SWCNTs) were separated by centrifuging, washed with deionized water for several times and dried in the oven at 313 K. The OX-SWCNTs were added to 1 g of cyanuric chloride, 25 mL dioxin and 25 mL xylene and shaken for 24 h. The resultant precipitates were mixed with 40 mL petroleum ether and remained at steady state for 24 h. Ch-SWCNTs were filtered and dried in oven for 2 h.

In the next step, 0.5 g of chitosan was gradually dissolved in 100 mL of acetic acid solution (2% v/v), then dried Ch-SWCNTs were added to the chitosan solution and centrifuged for 24 h at high speed. The Ch-SWCNTs were washed several times with 50 mL of 0.1 M buffer acetate sodium, 50 mL of 0.1 M NaCl solution, 20 mL methanol, and 100 mL deionized water, respectively, and finally, dried in an oven at 313 K for 2 h.

4. Adsorption Measurement

Batch adsorption experiments were carried out in 25 mL flask containing 20 $mg \cdot L^{-1}$ 5Fu, 2.5 mL of different buffers pH (3-10) Then, 0.005 adsorbent was added to 10 mL of the resulting solution. The mixture was stirred at a constant agitation rate for 60 min then the solid phases were separated by centrifugation. Drug concentration in the supernatant was determined by UV-Visible spectrometer at λ_{max}=269 nm. Adsorbed amount (q_t) of 5Fu per unit weight of Ch-SWCNTs at time t and removal efficiency (η(%)) of 5Fu onto the Ch-SWCNTs were calculated by Eqs. (1) and (2), respectively:

$$q_e = \frac{(C_0 - C_e)V}{W} \tag{1}$$

$$\eta(\%) = \frac{(C_0 - C_e)}{C_0} \times 100 \tag{2}$$

where, C_0 and C_e (mg/L) are the liquid-phase initial and equilibrium concentrations of the 5Fu, respectively. V (L) is the volume of the solution, and W (g) is the mass of nano-sorbent applied.

5. Kinetic and Thermodynamic Experiments

0.005 g of Ch-SWCNTs was added to 10 mL of the 5Fu solution (10 mgL^{-1}) in pH=4 at different contact times (2, 5, 10, 15, 30, 45, 60, 90 and 120 min) at 298 K under stirring at a constant agitation rate. The drug adsorption was determined in maximum adsorption wavelength (λ_{max}=269 nm) using UV-Vis spectrophotometer. The effect of changing the initial 5Fu concentrations (20, 40 mg/L) onto the Ch-SWCNTs were investigated at 298 K and q_t was calculated by Eq. (3).

$$q_t = \frac{(C_0 - C_t)V}{W} \tag{3}$$

where C_0 and C_t are the initial and equilibrium concentrations of 5Fu in solution (mg/L), respectively, V is the volume of solution (L), W is the adsorbent mass (g).

In isothermal experiments, 10 mL of 5Fu solution (at various concentrations of 2, 5, 10, 20, 30, 40, 60, 80, and 100 mg L^{-1}) was added to 0.005 g of functionalized adsorbent in 298 K and 1 h stirring. The same experiments were also repeated for 303, 308, and 313 K and q_e was calculated by Eq. (1).

RESULTS AND DISCUSSION

SWNCTs are exceptionally interesting from a fundamental research point of view. They are chemically stable, non-toxic, conduct electricity and mechanically strong. This research has benefits of combined SWNCTs and chitosan together. The chemically modified SWNCTs with chitosan possess both strong adsorption property and non-toxicity carried for interaction delivering of the drugs.

1. Characterization of the Adsorbents

1-1. FTIR Spectrum

To identify functional groups of materials, FTIR analysis was

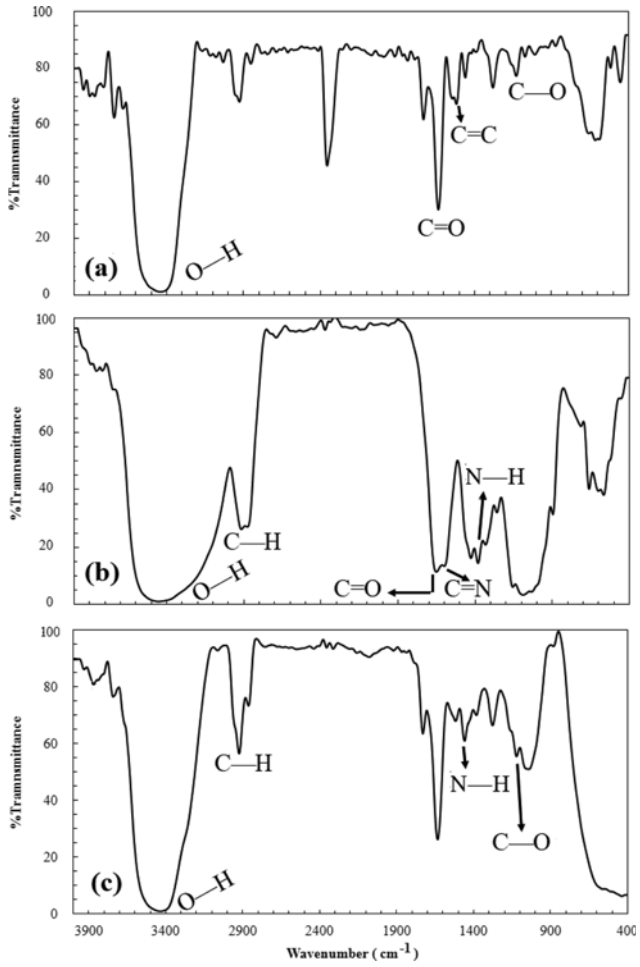

Fig. 1. FTIR spectrum of (a) OX-SWCNTs, (b) Ch-SWCNTs, and (c) Ch.

performed and the revealed spectra can be seen Fig. 1 and 2.

1-1-1. IR Spectrum of OX-SWCNTs, Ch and Ch-SWCNTs

a) The FTIR Spectrum of OX-SWCNT is shown in Fig. 1(a). The sharp peak in the range of 3,230-3,400 cm^{-1} and 1,400 cm^{-1} was attributed to stretching bond of O-H in -COH, -COOH groups. An absorption band in the range of 1,710-1,734 cm^{-1} belongs to C=O stretching vibrations of carboxylic acid groups. Conjugating of the double bond between C=O and C=C or the interaction between established C=C bonds and carboxylic acids appeared at 1,550-1,600 cm^{-1}. The peak at 1,110 cm^{-1} is corresponding to the C-O stretching vibration in alcoholic compounds.

b) The FTIR spectrum of Ch-SWCNTs is shown in Fig. 1(b). The band in the range 3,100-3,600 cm^{-1} was assigned to stretching vibration mode of O-H. The peak in the range 2,800-2,900 cm^{-1} was the characteristic bending vibrations of C-H groups. Those at 1,723 and 1,623 cm^{-1} were assigned to stretching vibration mode of C=O and C=N, respectively. The characteristic peak at 1,517 cm^{-1} is due to bending vibrations of N-H in the amine I band, the peak at 1,454 cm^{-1} originated from the symmetrical and asymmetrical stretch of -CH_2- groups.

c) The FTIR Spectrum of Ch is shown in Fig. 1(c). The observed peak of chitosan in the range of 3,400-3,600 cm^{-1} is due to the stretching vibration mode of O-H and NH_2 group, while the peak at 2,900 cm^{-1} is related to asymmetrical stretch of C-H, and the peak at 1,450 cm^{-1} is due to the N-H bending. Moreover, the peak at 1,100 cm^{-1} is ascribed the C-O stretching vibration.

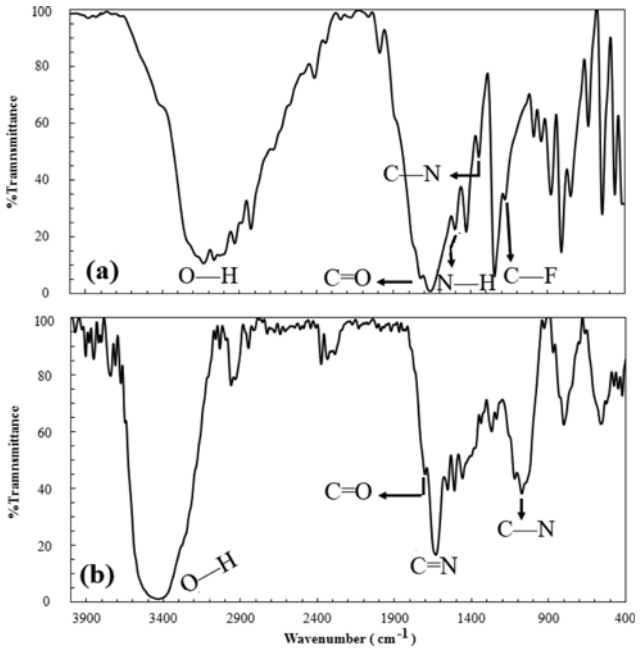

Fig. 2. FTIR spectrum of (a) 5Fu, and (b) 5Fu-Ch-SWCNTs.

1-1-2. IR Spectrum of the 5Fu, and 5Fu-Ch-SWCNTs

a) The FTIR spectrum of 5Fu (Fig. 2(a)) illustrates characteristic absorption bands of the functional groups of 5Fu in the range of 500-4,000 cm^{-1}. The broad absorption peaks in the range of 3,000-3,200 cm^{-1} represent the presence of an OH group, the peak at 1,656 cm^{-1} is related to bending vibrations of N-H (the amine I band). Also, the peak at 1,727 cm^{-1} could be assigned to the bending vibrations of C=O. The characteristic peaks at 1,240 and 1,351 cm^{-1} were corresponding to C-F and C-N vibrations in the structure of 5Fu, respectively.

b) The FTIR spectrum of 5Fu adsorbed onto Ch-SWCNTs (Fig 2(b)) indicates that 5Fu have been successfully loaded on Ch-SWCNTs by the formation of stretching vibration mode of C-N in the range 1,020-1,340 cm^{-1}. The strong peak at 1600, cm^{-1} was due to C=N and that in the range of 1,750-1,760 cm^{-1} was attributed to esteric functionalized C=O groups on SWCNTs.

1-2. BET Surface Area

The BET surface area was determined for chitosan, OX-SWCNTs and Ch-SWCNTs by N_2 adsorption-desorption isotherms at 77 K. Results indicated that chitosan has the minimum specific area of 2.91 m^2g^{-1}. The specific surface area of Ch-SWCNTs (111.10 m^2g^{-1}) is 90.88 m^2g^{-1} lower than that of OX-SWCNTs (201.9 m^2g^{-1}). Obviously, this comparison demonstrated coverage of chitosan on the surface of active SWCNTs.

1-3. Thermal Gravimetric Analysis (TGA)

Thermal stability of chitosan, OX-SWCNTs and Ch-SWCNTs was measured using TGA method (Fig. 3). Most of OX-SWCNTs weight losses occurred in the range of 550-750 °C. Maximum temperature of weight loss for Ch-SWCNTs is lower than pure SWCNTs,

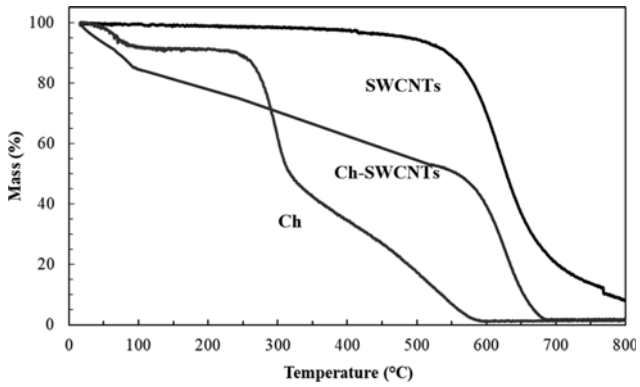

Fig. 3. Thermal gravimetric analysis of SWCNTs, Ch and Ch-SWCNTs.

so that Ch-SWCNTs lose more than 15% of their weight up to 100 °C due to the evaporation of physically adsorbed water. On the other hand, more than 30% weight reduction at 550 °C revealed the degradation of chitosan polymer. Therefore, it can be concluded that the chitosan biopolymer was successfully covered on active SWCNTs.

1-4. FE-SEM

Field emission scanning electron microscopy (FESEM) was used to study the morphology of Ch-SWCNTs, and the results are shown in Fig. 4. It can be seen that Ch-SWCNTs are cylindrical in shape, which is dispersed in chitosan matrix in a compressed form.

1-5. X-ray Diffraction (XRD)

Figs. 5(a), (b) and (c), show the XRD patterns of OX-SWCNTs, Ch-SWCNTs and chitosan, respectively. The intense and wide peak at 2θ=25.7° and the broad, peak at 2θ=43.19° for OX-SWCNTs (Fig. 5(a)), and Ch-SWCNTs (Fig. 5(b)) may be attributed to the (0 0 2) and (1 0 0) planes of graphitic carbon plates in the structure of SWCNTs. The XRD patterns of Ch-SWCNTs and Chitosan (Fig. 5(b) and (c)) show two relatively wide peaks at 2θ=10° and 20.2°, indicating the amorphous and crystal-like structure of chitosan polymer on the surface of SWCNTs.

2. Effect of pH on Adsorption

The effect of initial pH on the adsorption of 5Fu (20 mgL^{-1}) by Ch-SWCNTs composite was studied by varying pH over a range of 3-10 at 298 K. The qe values are shown in Fig. 6. It is obvious that higher adsorption capacity of 5Fu was achieved at pH=4. In pH<pk_a, it is as neutral species in aqueous solution. Furthermore,

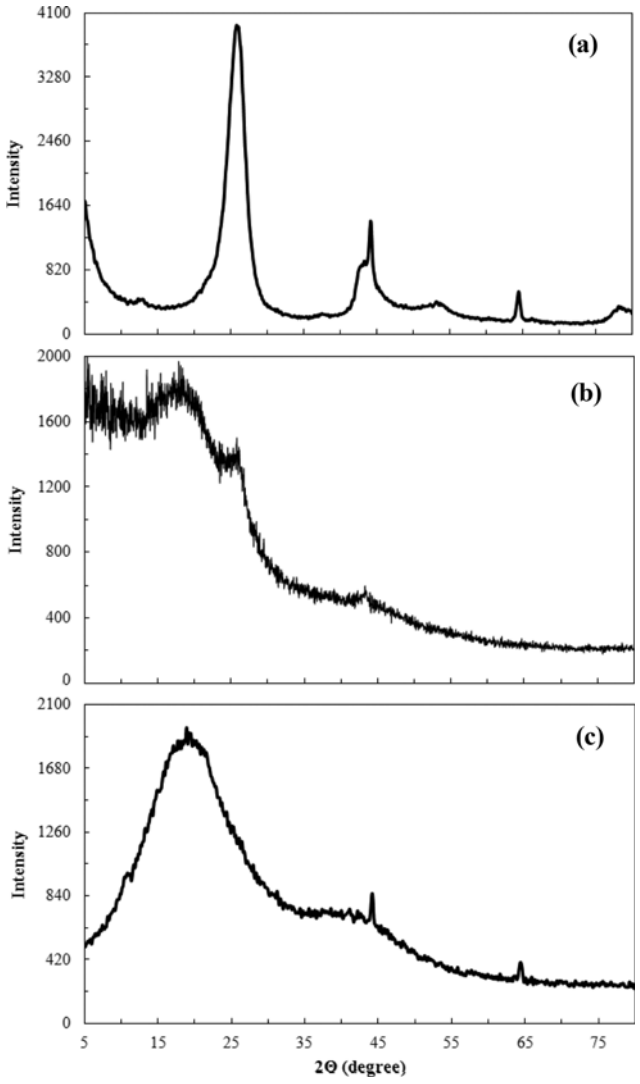

Fig. 5. XRD patterns of (a) OX-SWCNTs, (b) Ch and (c) Ch-SWCNTs.

the point of zero charge (pzc), of Ch-SWCNTs was reported to be approximately 4 [22], so the adsorbent has a neutral electric charge, too. Clearly, at pH=4 both the adsorbent and the adsorbate factors have no charge, which indicates that adsorption cannot take

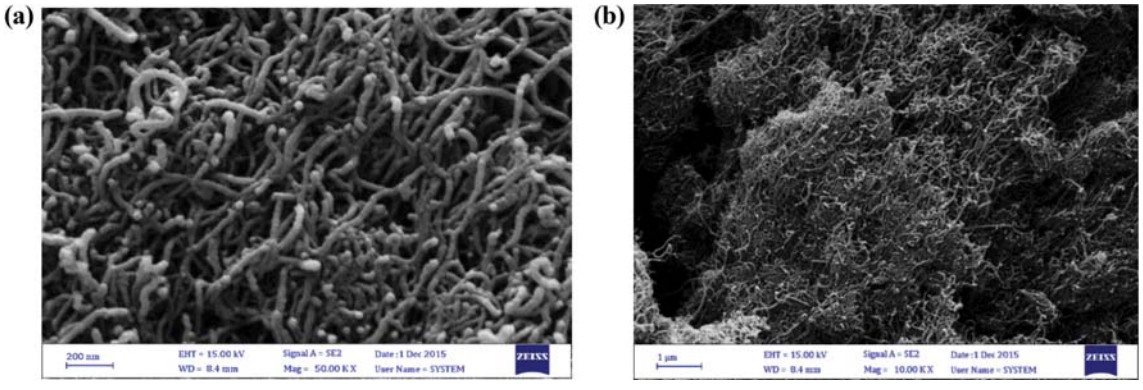

Fig. 4. SEM images of Ch-SWCNTs.

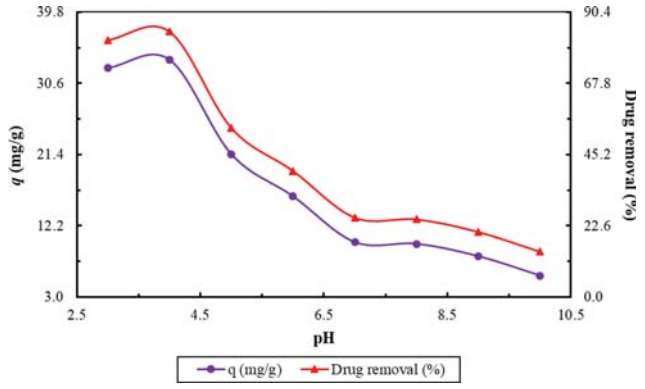

Fig. 6. Effect of pH on the adsorption and %removal of 5Fu by Ch-SWCNTs at 298 K and the initial drug concentration of 20 mg L^{-1}, shaking rate=150 rpm, t=120 min.

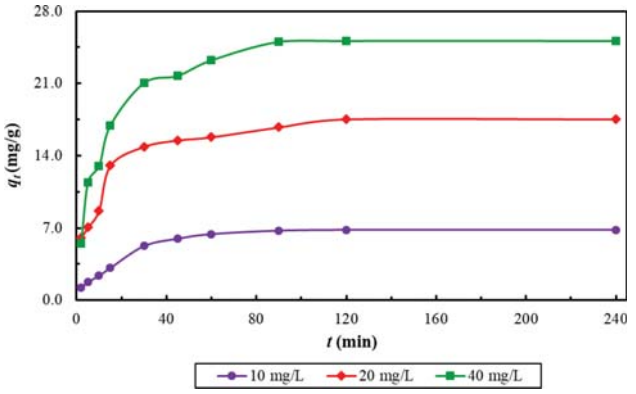

Fig. 7. Effect of initial 5Fu concentration on the adsorption of 5Fu by Ch-SWCNTs (conditions: 10, 20 and 40 mgL^{-1}, Ch-SWCNTs 0.005 g, pH 4, 150 rpm, and 298 K).

place through the electrostatic interactions; thus, the adsorption mechanism is mainly attributed to interaction of π-π electron donor-acceptor and hydrogen bonding by Ch-SWCNTs. NH groups of the drug possess lone pair electrons which participate in unestablished π system of electron-enriched rings of CNTs forming paired system. Meanwhile, carbonyl (CO) groups of the drug can accept lone pairs of amine (NH_2) and hydroxyl (OH) groups of chitosan. Moreover, establishing of hydrogen bonds between carbonyl and amine groups of the drug and oxygen and nitrogen atoms of chitosan is another important factor in drug adsorption by Ch-SWCNTs.

3. The Effect of Contact Time and Initial Concentration

Fig. 7 shows the effect of contact time on adsorption of 5Fu by Ch-SWCNTs at 298 K, pH=4 and 0.005 g adsorbent and various concentrations of the drug (10, 20 and 40 mgL^{-1}) in the range of 0 to 240 min. The adsorption capacity markedly increased within a few minutes, and then the trend rose slowly until adsorption equilibrium was reached within 90 minutes for all concentrations. The results reveal that the adsorption is rapid. The main reason for high adsorption rate in initial times is attributed to the availability of great number of adsorption sites or groups of adsorbents; after that the adsorption rate gradually decreased as these sites became progressively occupied by 5Fu.

In addition, the results presented that adsorption capacity at equilibrium is increased from 6.82 to 25.12 mg g^{-1}, by increasing the initial 5Fu concentration from 10 to 40 mgL^{-1}. At low initial concentrations of 5Fu, all free adsorption sites on the adsorbent surface are not filled, while in higher concentrations, each active adsorption site is surrounded by more drug [23].

4. Adsorption Kinetic

To obtain more information about the mechanism of 5Fu adsorption onto Ch-SWCNTs, the adsorptive kinetic data were described by various kinetic models such as pseudo-first-order rate (Eq. (4)), pseudo-second-order equation (Eq. (5)) [24], Elovich (Eq. (6)) and intra-particle diffusion (Eq. (7)).

Table 1. Nonlinear kinetic parameters of 5Fu adsorption onto Ch-SWCNTs at different concentrations*

Kinetics models	Parameters	Drug initial concentration (mg L^{-1})		
		10	20	40
Pseudo-first order	k_1 (min^{-1})	0.0464	0.0984	0.0889
	$q_{e,cal}$ (mg g^{-1})	6.8287	16.519	23.955
	R^2	0.9978	0.9914	0.9947
	$q_{e,exp}$ (mg g^{-1})	6.8156	17.5319	25.1196
Pseudo- second order	k_2 (g $mg^{-1}min^{-1}$)	0.0072	0.0077	0.0046
	$q_{e,cal}$ (mg g^{-1})	7.8536	18.068	26.4404
	R^2	0.9955	0.9954	0.9985
	$q_{e,exp}$ (mg g^{-1})	6.8156	17.5319	25.1196
Intraparticle diffusion	k_i (mg $g^{-1}min^{-1/2}$)	0.4522	0.8556	1.3265
	C (mg g^{-1})	1.6349	7.5829	9.9854
	R^2	0.9576	0.9756	0.9709
Simplified Elovich	α (mg $g^{-1}min^{-1}$)	1.2448	11.0926	10.941
	β (g mg^{-1})	0.6842	0.3546	0.2254
	R^2	0.9871	0.9931	0.9944

*Conditions: 5Fu 10, 20 and 40 mgL^{-1}, Ch-SWCNTs 0.005 g, pH 4, 150 rpm, and 298 K

$$\log(q_e - q_t) = \log q_e - \frac{k_1}{2.303}t \quad (4)$$

$$\frac{t}{q_t} = \frac{1}{k_2 q_{e2}^2} + \frac{1}{q_{e2}}t \quad (5)$$

$$q_t = k_i t^{1/2} + C \quad (6)$$

$$q_t = \frac{1}{\beta}\ln(\alpha\beta) + \frac{1}{\beta}\ln t \quad (7)$$

where, q_e and q_t are the values of amount adsorbed per unit mass at equilibrium and at instant of time t (min). K_1, K_2 and K_i are the pseudo-first-order, pseudo second-order, and intra-particle diffusion adsorption rate constant, respectively, and c_i is related to the thickness of the boundary layer. α and β represent the initial adsorption rate and the desorption coefficient, respectively.

The parameter values for each system are listed in Table 1; it was found that the kinetic behavior of 5Fu adsorption onto the Ch-SWCNTs is more appropriately described by the pseudo-second-order kinetic model due to a higher correlation coefficient (R^2). As we can see in Fig. 8, the experimental data were fitted to the pseudo-second-order theoretical model. This result confirms that kinetic adsorption of 5Fu on Ch-SWCNTs followed the pseudo-second-order model. Thus, the parameter values calculated adsorption capacity (q_e) by the pseudo-second-order model are in good agreement with the experimental values ($q_{e,exp}$).

5. Adsorption Isotherm

Studying equilibrium adsorption isotherms provides valuable information to describe the interactive behavior of adsorbent and adsorbate. In this research, 5Fu adsorption on OX-SWCNTs and Ch-SWCNTs was analyzed using the Langmuir, Freundlich, Temkin and Dubinin-Radushkevich (D-R) isotherm models (Fig. 9, 10).

5-1. Langmuir Isotherm

This isotherm is attributed to monolayer adsorption on the homogeneous surface containing a finite number of identical sorption sites and lack of movement with a constant adsorption energy. Langmuir isotherm is as follows by Eq. (8):

$$\frac{C_e}{q_e} = \frac{1}{K_l q_{max}} + \frac{C_e}{q_{max}} \quad (8)$$

where q_{max} represents maximum capacity of the adsorbent (mg g^{-1}); and K_l is the Langmuir adsorption constant (L mg^{-1}) [25].

The main characteristic of the Langmuir isotherm is represented by dimensionless equilibrium parameter (R_l). R_L shows the type of the isotherm to be either unfavorable if (R_L>1), linear if (R_L=1), favorable if (0<R_L<1), and irreversible if (R_L<1), (Eq. (9)):

$$R_l = \frac{1}{1 + K_l C_0} \quad (9)$$

where C_0 is the highest drug initial concentration [26].

5-2. Freundlich Isotherm

This model is applied to multilayer adsorption on the heterogeneous surfaces with intra-molecular interaction of adsorption. Linear form of this model is presented by Eq. (10).

$$q_e = K_F C_e^{1/n} \quad (10)$$

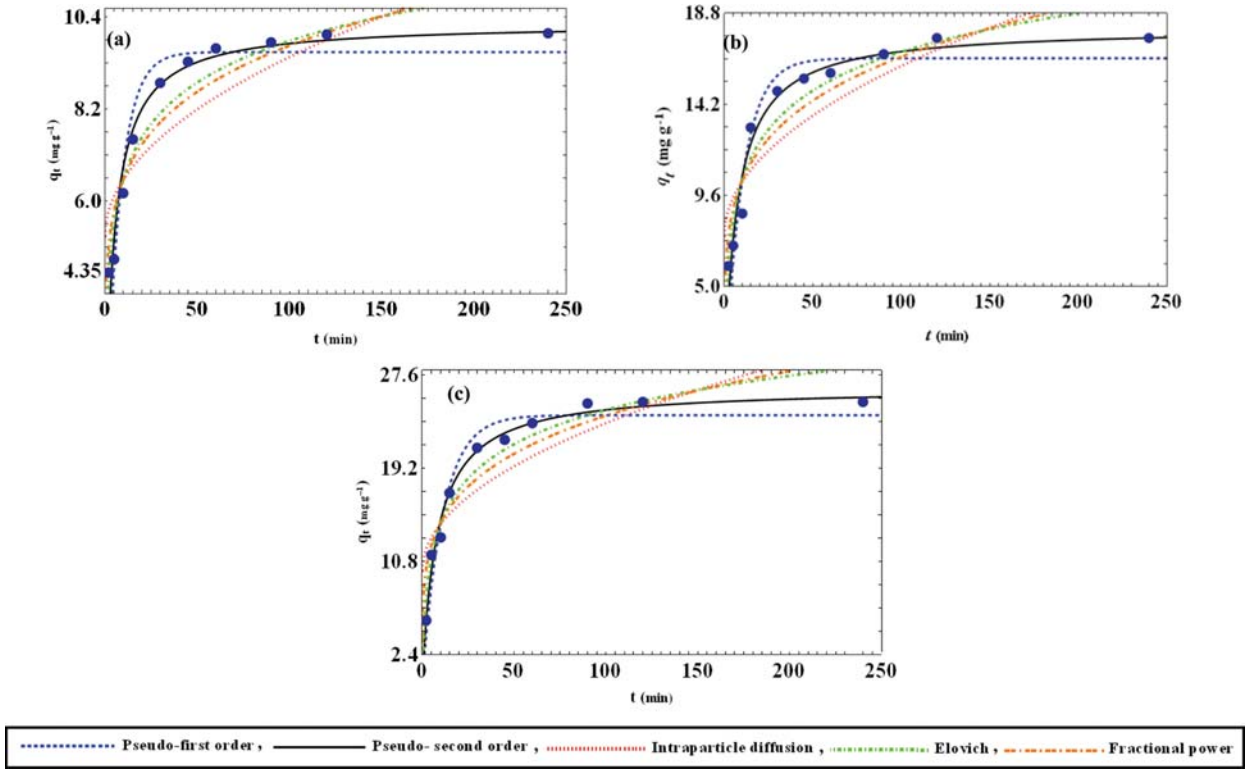

Fig. 8. Nonlinear form of kinetic models for adsorption of 5Fu by Ch-SWCNTs at different concentrations of 5Fu (a) 10 mgL^{-1}, (b) 20 mgL^{-1} and (c) 40 mgL^{-1}.

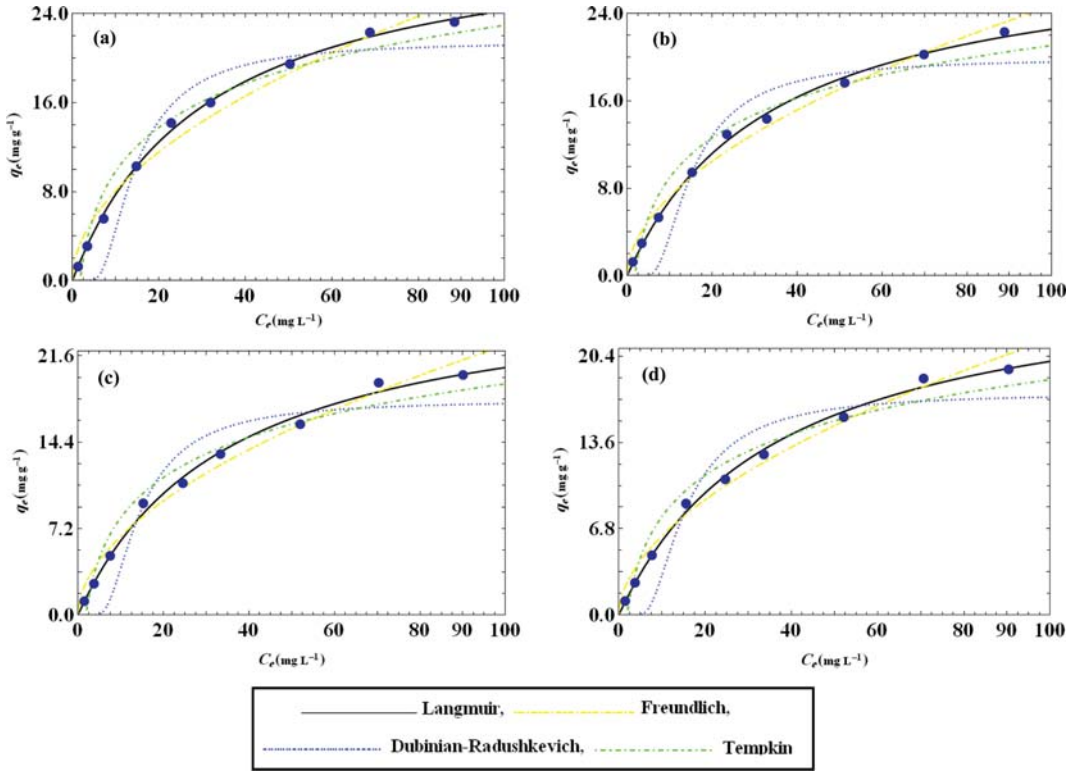

Fig. 9. Nonlinear form of two parameter isotherm models for adsorption of 5Fu by Ch-SWCNTs at (a) 298 K, (b) 303 K, (c) 308 K and (d) 313 K (The dark circle shows experimental data).

Table 2. Nonlinear isotherm parameters of 5Fu adsorption onto Ch-SWCNTs at different temperature*

Isotherm models	Parameters	Temperature (K)			
		298	303	308	313
Langmuir	q_m (mg g^{-1})	31.7748	30.2091	27.8262	27.3495
	K_L (L mg^{-1})	0.0322	0.0294	0.0286	0.0271
	R_L	0.2367	0.2538	0.2588	0.2693
	R^2	0.9995	0.9994	0.9985	0.9990
Freundlich	K_F (mg$^{1-\frac{1}{n}}$L$^{\frac{1}{n}}$g^{-1})	2.4335	2.124	1.9181	1.7915
	n	1.9232	1.8777	1.8705	1.8454
	R^2	0.9926	0.9956	0.9947	0.9954
Dubinin-Radushkevich	Q_m (mg g^{-1})	21.4901	19.9043	17.903	17.494
	K (mol^2 kJ^{-2})	2.7649×10^{-5}	2.9304×10^{-5}	2.551×10^{-5}	2.794×10^{-5}
	R^2	0.9774	0.9721	0.9697	0.9954
Temkin	K_T (L mg^{-1})	0.5591	0.5529	0.5345	0.5244
	b (J g mol^{-1} mg^{-1})	434.855	480.317	529.165	556.006
	R^2	0.9894	0.9884	0.9879	0.9871

*Conditions: 5Fu 20 mgL^{-1}, Ch-SWCNTs 0.005 g, pH 4, 150 rpm, t 120 min

where K_F is Freundlich constant (L mg^{-1}), which indicates the relative adsorption capacity of the adsorbent; n is the heterogeneity factor. Values of 1<n<10 suggest favorable adsorption [27].

5-3. Temkin Isotherm

Temkin isotherm considers the effect of interaction between adsorbent-adsorbed on adsorption isotherms. Temkin relation is presented by Eq. (11).

$$q_e = B_T \ln K_T + B_T \ln C_e \quad (11)$$

where B_T=RT/b, b is the Temkin constant dependent on heat of sorption (J mol^{-1}), and B_T and K_T are the Temkin isotherm constants (L g^{-1}), T is the absolute temperature (K) and R is the uni-

versal gas constant (8.314 J $mol^{-1}K^{-1}$).

5-4. Dubinin-Radushkevich (D-R) Isotherm

According to this model (Eq. (12)), the surface is not assumed to be homogeneous and adsorption potential is not considered constant.

$$q_e = Q_m \exp(-K\varepsilon^2) \quad (12)$$

In this equation, K is the constant of adsorption energy, Q_m is the theoretical saturation capacity and ε represents Polanyi potential.

Comparison of the regression coefficient (R^2) of different isotherm models shows that the Langmuir isotherm has a good agreement between the isotherm parameters and experimental values. Moreover, values of $0<R_L<1$ indicate that adsorption is favorable and the homogeneous distribution of active sites on the surface of Ch-SWCNTs.

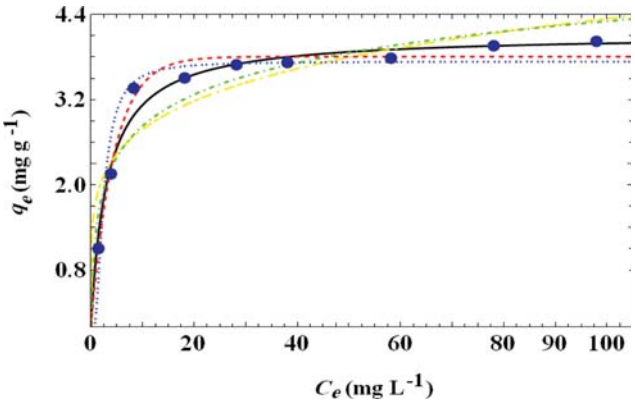

Fig. 10. Nonlinear form of two parameter isotherm models for adsorption of 5Fu by SWCNTs at 298 K (The dark circle shows experimental data).

Table 3. Nonlinear isotherm parameters of 5Fu adsorption onto SWCNTs at different temperature*

Isotherm models	Parameters	Temperature (K)
		298
Langmuir	q_m (mg g^{-1})	4.1181
	K_L (L mg^{-1})	0.3137
	R_L	0.0309
	R^2	0.9979
Freundlich	K_F (mg $^{1-\frac{1}{n}}$ $L^{\frac{1}{n}}$ g^{-1})	1.7836
	n	5.1811
	R^2	0.9851
Dubinin-Radushkevich	Q_m (mg g^{-1})	3.7365
	K (mol^2 kJ^{-2})	1.0223×10^{-6}
	R^2	0.9936
Temkin	K_T (L mg^{-1})	8.2368
	b (J g mol^{-1} mg^{-1})	3866.67
	R^2	0.9909

*Conditions: 5Fu 20 mgL^{-1}, SWCNTs 0.005 g, pH 4, 150 rpm, t 120 min

From Table 2 and Fig. 9, the maximum adsorption capacity (q_m) of Langmuir model decreases from 31.77 to 27.35 mg g^{-1} with increase in temperature and this indicates an exothermic adsorption process.

Nonlinear form of two parameter isotherm models for adsorption of 5Fu by OX-SWCNTs at different temperature is shown in Fig. 10, and the adsorption capacity of 5Fu on OX-SWCNTs is given in Table 3 (at 298 K, q_m is 4.12 mg g^{-1}), A comparison of the results obtaining 5Fu adsorption on OX-SWCNTs and Ch-SWCNTs confirms enhancement of adsorption capacity.

The main reason for enhanced adsorption capacity in Ch-SWCNTs adsorbent can be attributed to the presence of frequent function abundant carboxyl and amine groups on the surface of chitosan.

6. Thermodynamic Parameters of Adsorption

In this paper, thermodynamic parameters of 5Fu adsorption on Ch-SWCNTs, change in standard Gibb's free energy (ΔG^o), enthalpy (ΔH^o) and entropy (ΔS^o) were evaluated. Values of these parameters were calculated by Eq. (13), (14), and (15), respectively [28].

$$K_l = \frac{q_e}{C_e} \quad (13)$$

$$\Delta G^o = -RT\ln K_l \quad (14)$$

$$\ln K_l = \frac{\Delta S^o}{R} - \frac{\Delta H^o}{RT} \quad (15)$$

Table 4. Thermodynamic parameters of 5Fu adsorption onto Ch-SWCNTs at different temperature*

Temperature (K)	ΔH (J mol^{-1})	ΔS (J $mol^{-1}K^{-1}$)	TΔS (kJ mol^{-1})	ΔG (kJ mol^{-1})
298.15	−8608.32	−0.0925	−27.5789	−8.5807
303.15			−28.0414	−8.5803
308.15			−28.5039	−8.5794
313.15			−28.9664	−8.5784

*Conditions: 5Fu 20 mgL^{-1}, Ch-SWCNTs 0.005 g, pH 4, 150 rpm, t 120 min

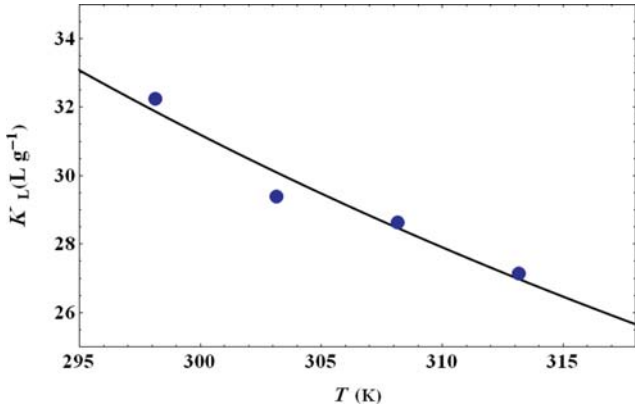

Fig. 11. The van't Hoff plot adsorption of 5Fu by Ch-SWCNTs at different temperature (conditions: 5Fu 20 mgL^{-1}, Ch-SWCNTs 0.005 g, pH 4, 150 rpm).

Adsorption experiments were conducted at 298, 303, 308 and 313 K to calculate thermodynamic parameters of 5Fu adsorption on Ch-SWCNTs. Values of thermodynamic parameters are presented in Table 4. The plot of K_l as a function of T yields ΔH^o and ΔS^o (Fig. 11). Negative values of ΔH^o suggest that the adsorption process of 5Fu on Ch-SWCNTs is exothermic, hence an increase in temperature reduces adsorption rate. Regarding adsorption heat (ΔH^o=−8,608.32 J mol^{-1}), indicates physisorption process [29] Negative ΔG^o indicates that adsorption is spontaneous. Generally, the change of free energy for physisorption is between 0 and 20 kJ mol^{-1}. Positive ΔS^o values suggest increased randomness during the adsorption process.

CONCLUSION

The prospective application of Ch-SWCNTs nano composite for 5Fu adsorption in aqueous solutions has been illustrated in this study. The prepared composite possesses abundant functionalized oxygen groups, such as carboxyl, hydroxyl and amine. Prepared adsorbent was characterized using various techniques such as FTIR, FESEM, TGA, BET and XRD. Adsorption of 5Fu is dependent on pH, temperature and initial concentration of the drug. Adsorption data were consistent with the pseudo second-order kinetic model and Langmuir isotherm model. Efficiency of Ch-SWCNTs in adsorbing 5Fu is more than OX-SWCNTs. Maximum adsorption capacity (q_m) based on Langmuir model was 31.77 mg g^{-1} at 298 K with pH 4. The values of thermodynamic parameters (ΔG^o, ΔH^o and ΔS^o) indicated that the adsorption process was spontaneous and exothermic with decreasing randomness during the process.

REFERENCES

1. M. Ghasemi Nooreini and H. Ahmad Panahi, *Int. J. Pharm.*, **512**, 178 (2016).
2. A. Heydarinasab, H. Ahmad Panahi, H. Nematzadeh, E. Moniri and S. Nasrollahi, *Monastsh. Chem.*, **146**, 411 (2015).
3. H. Ahmad Panahi and S. Nasrollahi, *Int. J. Pharm.*, **476**, 70 (2014).
4. H. Ahmad Panahi, Y. Tavanaei, E. Moniri and E. Keshmirizadeh, *J. Chromatogr. A*, **1345**, 37 (2014).
5. H. Ahmad Panahi and H. Alaei, *Int. J. Pharm.*, **476**, 178 (2014).
6. Y. Hu, D. H. Fine, E. Tasciotti, A. Bouamrani and M. Ferrari, *Nanomed. Nanobiotechnol.*, **3**, 11 (2011).
7. C. Menard-Moyon, E. Venturelli, C. Fabbro, C. Samori. T. Da Ros, K. Kostarelos, M. Prato and A. Bianco, *Expert Opin. Drug Discovery*, **5**, 691 (2010).
8. R. H. Baughman, A. A. Zakhidov and W. A. de Heer, *Science*, **297**, 787 (2002).
9. A. Bianco, K. Kostarelos and M. Prato, *Curr. Opin. Chem. Biol.*, **9**, 674 (2005).
10. P. Liu, *Ind. Eng. Chem. Res.*, **52**, 13517 (2013).
11. D. J. Lim, M. Sim, L. Oh, K. Lim and H. Park, *Arch. Pharm. Res.*, **37**, 43 (2014).
12. Z. Liu, J. T. Robinson, S. M. Tabakman, K. Yang and H. Dai, *Mater. Today*, **14**, 316 (2011).
13. A. Khazaei, M. N. S. Rad and M. K. Borazjani, *Int. J. Nanomed.*, **5**, 639 (2010).
14. Z. Liu, K. Chen, C. Davis, S. Sherlock, Q. Z. Cao, X. Y. Chen and H. J. Dai, *Cancer Res.*, **68**, 6652 (2008).
15. Z. Liu, A. C. Fan, K. Rakhra, S. Sherlock, A. Goodwin, X. Y. Chen, Q. W. Yang, D. W. Felsher and H. J. Dai, *Angew. Chem., Int. Ed.*, **48**, 7668 (2009).
16. M. Khalaj Moazen and H. Ahmad Panahi, *J. Sep. Sci.*, **40**(5), 1125 (2017).
17. W. Fan, W. Yan, Z. Xu and H. Ni, *Colloids Surf., B: Biointerfaces*, **95**, 258 (2012).
18. K. S. C. R. dos Santos, J. F. J. Coelho, P. Ferreira, I. Pinto, S. G. Lorenzetti, E. I. Ferreira, O. Z. Higa and M. H. Gil, *Int. J. Pharm.*, **310**, 37 (2006).
19. E. Dadvar, R. R. Kalantary, H. Ahmad Panahi and M. Peyravi, *J. Chem.*, **2017**, 1 (2017).
20. X. K. Zhang, L. J. Meng, Q. H. Lu, Z. F. Fei and P. J. Dyson, *Biomaterials*, **30**, 6041 (2009).
21. J. Li, H. Sun and Y. D. Dai, *Chin. Phys. Lett.*, **27**, 38104 (2010).
22. Y. Zhan, L. Pan, C. Nie, Li, H. Li and Z. Sun, *J. Alloys Compd.*, **509**, 5667 (2011).
23. N. K. Amin, *J. Hazard. Mater.*, **165**, 52 (2009).
24. Y. S. Ho and G. Mckay, *Process Biochem.*, **34**, 451 (1999).
25. I. Langmuir, *J. Am. Chem. Soc.*, **40**, 1361 (1918).
26. K. R. Hall, L. C. Eagleton, A. Acrivos and T. Vermeulen, *Ind. Eng. Chem. Fundam.*, **5**, 212 (1966).
27. C. Namasivayam, R. Jeyakumar and R. T. Yamuna, *Waste Manage.*, **14**, 643 (1994).
28. T. K. Naiya, A. Bhattacharya and S. K. Das, *J. Colloid Interface Sci.*, **333**, 14 (2009).
29. W. Konicki, I. Pełech, E. Mijowska and I. Jasińska, *Chem. Eng. J.*, **210**, 87 (2012).